Journal of Machine Construction and Maintenance
PROBLEMY EKSPLOATACJI
QUARTERLY
ISSN 1232-9312 4/2017 (107)
p. 53–61

Andrzej KUREK, Justyna KOZIARSKA, Krzysztof KLUGER, Tadeusz ŁAGODA
Opole University of Technology, Faculty of Mechanical Engineering, Poland
t.lagoda@po.opole.pl

FATIGUE LIFE OF 2017A-T4 ALUMINIUM ALLOY UNDER DIFFERENT TYPES OF STRESS

Key words: fatigue, plane bending, plastic strain, tension-compression, uniaxial loading.

Abstract: The paper presents a comparison of the results of fatigue life experimental results on 2017A-T4 aluminium alloy with tests performed under two types of stress, i.e. tensile-compressive (both strain-controlled and energy parameter controlled) and oscillatory bending (bending moment controlled). The results are obtained by applying the Basquin's stress-life equation and strain-life equations, including Kandil's equation, Langer's equation, and the authors' own equation. On the basis of own experimental studies and the relevant physical relations, the stress and strain amplitudes occurring in bent rods under smooth specimens were calculated according to the elastoplastic model. The results were then used to compare both types of loads with different types of control.

Charakterystyki zmęczeniowe stopu aluminium 2017A-T4 uzyskane przy różnych sposobach obciążenia

Słowa kluczowe: zmęczenie, gięcie płaszczyzny, odkształcenie plastyczne, jednoosiowe obciążenie.

Streszczenie. W pracy przedstawiono porównanie wyników eksperymentalnych badań zmęczeniowych stopu aluminium 2017A-T4 przeprowadzonych dla dwóch rodzajów obciążeń: rozciągania-ściskania (przy sterowaniu odkształceniem oraz parametrem energetycznym) i zginania wahadłowego (przy kontrolowanym momencie zginającym), stosując do tego charakterystyki zmęczeniowe: naprężeniową Basquina, oraz odkształceniowe: Mansona-Coffina-Basquina, Kandila, Langera i własną. Wykorzystując własne badania eksperymentalne oraz odpowiednie związki fizyczne, dokonano przeliczenia amplitud naprężenia i odkształcenia, występujących w zginanych prętach bez karbu geometrycznego według modelu ciała sprężysto-plastycznego. Wyniki posłużyły do porównania obu rodzajów obciążeń przy różnym sposobie sterowania.

NOMENCLATURE

A, m – constants in the regression model,
b – fatigue life exponent,
c – exponent of plastic fatigue strain,
E – Young's modulus,
K' – cyclic strength coefficient,
n' – cyclic strengthening exponent,
N_f – fatigue life (in cycles),
$2N_f$ – the number of loading recurrences (semi-cycles),
R – maximum height (radius in case of round component (rod)),
x – the distance from bending plane,
$\varepsilon_{a,t}$ – total strain amplitude expressed as the sum of the amplitudes of elastic strain $\varepsilon_{a,e}$ and plastic strain $\varepsilon_{a,p}$,
ε'_f, – coefficient of plastic fatigue strain,
σ'_f, – fatigue life coefficient,
σ_a – stress amplitude.

Introduction

Fatigue tests involving a low number of cycles (i.e. under Low Cycle Fatigue regime) are usually conducted in strain control, while tests with a high number of cycles (i.e. under High Cycle Fatigue regime) are usually conducted in strength-controlled environment. The tests under tensile-compressive stress and torsion are performed by employing thin specimens. However, in the case of bending or torsion of thick specimens, which are employed in numerous experimental studies, bending moment or torque is the controlled parameter, and this kind of tests is mostly conducted under High Cycle Fatigue regime [1].

In the literature, the fatigue phenomenon is usually described by using fatigue models, expressed both in terms of stress and strain for tension-compression. However, a considerable number of fatigue tests reported in the literature refers to bending – usually, oscillatory bending or, less frequently, rotational bending. Due to the stress (strain) gradient occurring specimen while bending, not all models commonly used for tension-compression can be used for this type of loadings. There are only a handful of studies in the literature which compare those loadings, and those that are available refer to stress-life models [2–4], but there are no such comparisons for strain-life models. According to the tests reported in the published studies, at the level of fatigue limit, the load type does not affect the fatigue life; whereas, at level of fatigue strength with bending, higher strength is obtained with respect to tension-compression. The study in [5] shows the impact of the change of the bending plane on the fatigue strength, as compared to fixed bending plane (oscillatory bending).

In this study, the authors compared the strain-life calculated for tension-compression under both controlled strain and energy parameter, and for oscillatory bending at controlled bending moment for samples of 2017A-T4 T4 aluminium.

1. Strain-life models

The basic strain-life fatigue model is the Manson-Coffin-Basquin (MCB**)** equation [6, 7], which is given the following form:

$$\varepsilon_{a,t} = \varepsilon_{a,e} + \varepsilon_{a,p} = \frac{\sigma'_f}{E}\left(2N_f\right)^b + \varepsilon'_f\left(2N_f\right)^c \tag{1}$$

where $\varepsilon_{a,t}$ is the amplitude of total strain, $\varepsilon_{a,e}$ is the amplitude of elastic strain, and $\varepsilon_{a,p}$ is the amplitude of plastic strain.

Originally, the **MCB** equation was formulated for tension-compression on the basis of strain and stress amplitudes and the number of cycles required to destroy the specimen.

Eq. (1) can be used to graph the **MCB** curve only when it is possible to separately determine the amplitude of both the elastic component $\varepsilon_{a,e}$ and plastic component $\varepsilon_{a,p}$ from the total strain $\varepsilon_{a,t}$.

For cyclical loads we have the following:

$$\varepsilon_{a,e} = \frac{\sigma_a}{E} \tag{2}$$

and

$$\varepsilon_{a,p} = \varepsilon_{a,t} - \varepsilon_{a,e} \tag{3}$$

Another aspect was reported in [8], where the authors showed that the role of plastic strain in Eq. (1) depends on the fatigue strength, i.e. *c* is not a constant value.

Furthermore, several authors proposed different empirical models where the total strain amplitude was dependent on the number of cycles. Those proposals find application when it is not possible to separate the elastic and the plastic components of the total strain, such as by Langer [9], which is used in numerous studies and popularised by Manson [10, 11] and Crop [12]:

$$logN_f = A - B\log\left(\varepsilon_{a,t} - C\right) \tag{4}$$

where A, B, C are constant values for the given material.

Other proposals include Kandil's equation [13] and Gorasek's equation [14] in the following form:

$$\log\,\varepsilon_{a,t} = A - B\log\left(N_f\right) + C\,log^2\left(N_f\right) \tag{5}$$

where A, B, C are constant values for the given material.

Under bending, it is not possible to separate the elastic and plastic components; therefore, it is not possible to apply Eq. (1). However, Eqs (4) or (5) can be applied, or another empirical form of the strain-life. The proposal of the authors is a combination of Eqs. (4) and (5), given by the following form:

$$log\left(\varepsilon_{a,t} - D\right) = A - B\log\left(N_f\right) + C\,log^2\left(N_f\right) \tag{6}$$

where A, B, C, D are constant values for the given material.

The new form of fatigue equation, here proposed by the authors, requires determining the four material constants, which is A, B, C and D, similarly to the widely applied MCB (see Eq. (1)).

2. Strain and stress in element under variable loading

The correlation between the amplitudes of stress and strain is described by the Ramberg-Osgood equation [15] in the following form:

$$\varepsilon_{a,t} = \varepsilon_{a,e} + \varepsilon_{a,p} = \frac{\sigma_a}{E} + \left(\frac{\sigma_a}{K'}\right)^{\frac{1}{n'}} \tag{7}$$

The literature has thus far failed to provide a simple method of determining strain and stress according to the elastic-plastic model for elements, without geometric notches, and subjected to bending moment. However, it has been experimentally confirmed that, in the scope of small strains, the distribution of normal strain in a bent section is linear and this can be written as follows:

$$\varepsilon_a(x) = \varepsilon_{a\max}\frac{x}{R} \tag{8}$$

where x is the distance from the plain of bending, and R is the radius of specimen.

The crucial requirement to be met here is that the normal strain, which occurs both in elastic and in plastic-elastic model, must balance out the specified bending moment M_b , i.e.:

$$M_b = \int_S \sigma(x,y)x dS \tag{9}$$

where y is the distance across specimen, and S is the area of cross section of the specimen.

Therefore, in a section of a bent element, a system of three equations that are (7), (8), and (9), must be satisfied jointly. Figure 1 illustrates the distribution of stress and strain under bending.

Figure 2 shows the values in the specimen section, which are necessary to calculate the distribution of strain and bending moment according to the elastoplastic body model.

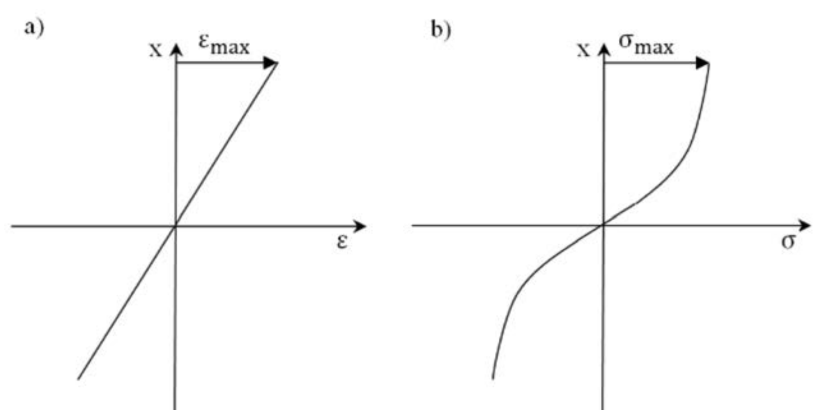

Fig. 1. Distribution of strain (a) and stress (b) in a bent element

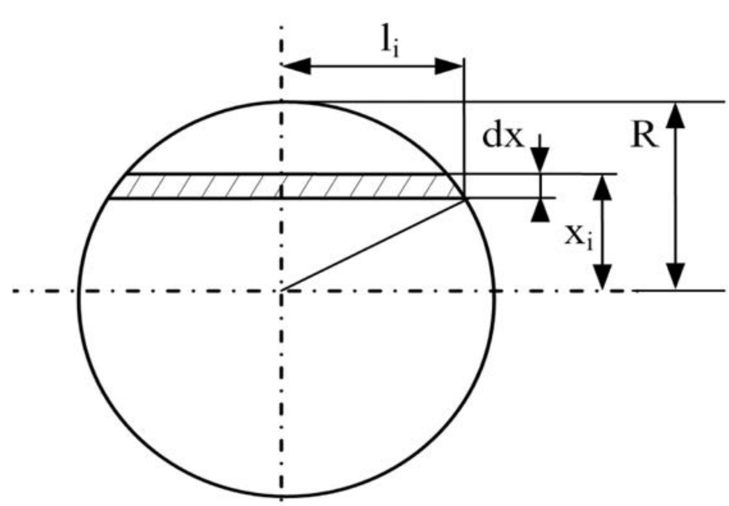

Fig. 2. Section of bent sample

3. Experimental campaign

The experimental studies were performed on 2017A-T4 aluminium alloy samples. The chemical composition of the analysed material is listed in Table 1, while its mechanical and fatigue properties are listed in Tables 2 and 3, respectively.

Table 1. Chemical composition of analysed material, % (Al – the rest)

Cu	Mg	Mn	Si	Fe	Zr+Ti	Zn	Cr	other total	other separately
3.5 –4.5	0.4 –1.0	0.4 –1.0	0.2 – 0.8	<0.7	<0.25	<0.25	<0.10	<0.15	<0.05

Table 2. Mechanical properties of analysed material

E, GPa	R_e, MPa	R_m, MPa	A_5, %	ν
72	395	545	21	0.32

Table 3. Fatigue properties of analysed material

ε'_f	c	σ'_f, MPa	b	K', MPa	n'
1.879	-0.988	643	-0.065	617	0.066

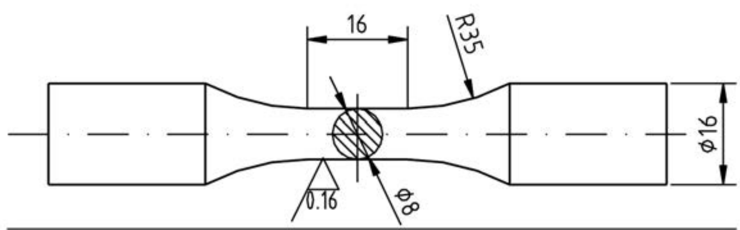

Fig. 3. Tension-compression sample geometry

Three types of fatigue tests were performed. Each tensile-compressive test was strain-controlled, i.e. ε_a = const [16], and the samples had the geometric features illustrated in Fig. 3.

The second type of tests was oscillatory bending, in which a constant bending moment amplitude was achieved (M_{ga}= const) [17, 18, 19, 20], i.e. by assuming a fixed stiffness *EI*, a constant amplitude of nominal stress was achieved (adopting the perfectly elastic body model), according to the following formula:

$$\sigma_{an} = \frac{M_{ga}}{w_x} \tag{10}$$

In consideration of the above, it was necessary to apply the elastoplastic body model in order to determine the stress and strain amplitudes, the values of which would be closer to actual values. The tests were performed on diabolo shaped solid samples shown in Fig. 4. As a result, Basquin's equation was obtained according to the following formula:

$$\log N_f = 21.87 - 7.03 \log \sigma_{an} \tag{11}$$

where σ_{an} is nominal amplitude of stress.

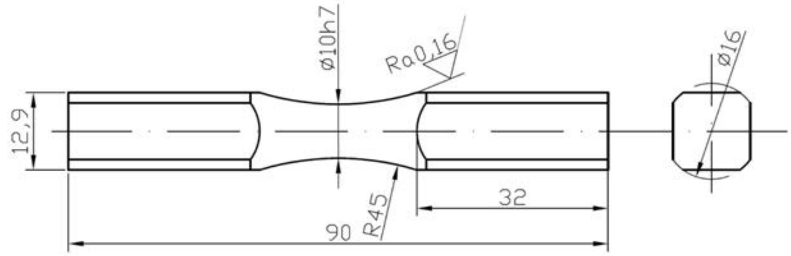

Fig. 4. Sample geometry applied for oscillatory bending

The third tests type [21] was tension-compression at a constant amplitude of energy parameter (W_a = const) [22], where

$$W(t) = 0.25 \{ |\sigma(t)| \varepsilon(t)+\sigma(t) |\varepsilon(t)| \} \qquad (12)$$

which in load amplitude-based form eventually gives

$$W_a = 0.5\sigma_a \varepsilon_a \qquad (13)$$

where W_a is the amplitude of the strain energy parameter.

A comprehensive analysis yielded of the energy parameter, stress and strain, and a stabilised strain amplitude on specimens similar to those tested in strain-controlled loading (Fig. 3).

Tests with controlled moment (nominal stress) were conducted on the station illustrated on Fig. 5. The geometric form of samples used in the tests is provided on Fig. 4.

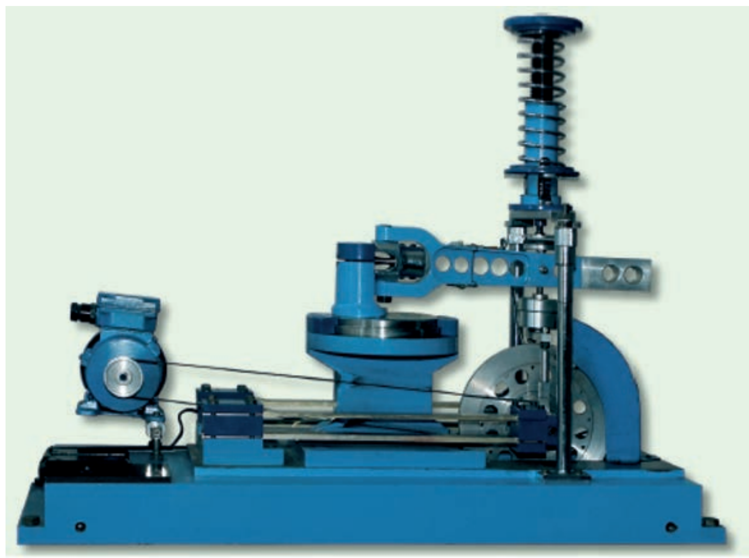

Fig. 5. Fatigue testing station with controlled bending moment

4. Results and discussion

The results of all experiments are provided in Table 4 (for a single-axis tension-compression under strain control), Table 5 (for oscillatory bending with controlled bending moment), and Table 6 (for single-axis tension-compression, with the stress-strain parameter control).

Table 4. Results of fatigue tests for tension-compression under strain control

No.	$\varepsilon_{a,t}$, ‰	N_{exp}, cycles
1	5	4720
2	5	3600
3	6	2100
4	6	1550
5	7	700
6	7	550
7	8	5360
8	8	370
9	10	240
10	10	150

Table 5. Results of fatigue tests for oscillatory bending under controlled moment (nominal stress)

No.	σ_{an}, MPa	N_{exp}, cycles
1	154	6 271 200
2	154	>10 000 000
3	154	>10 000 000
4	168	944 800
5	168	1 978 000
6	168	4 986 000
7	178	781 000
8	178	680 000
9	178	447 500
10	192	467 000
11	192	1 502 000
12	192	334 000
13	204	254 000
14	204	531 000
15	204	443 000
16	227	159 000
17	227	223 000
18	227	98 000
19	243	203 000
20	243	64 000
21	243	165 000

Table 6. Results of fatigue tests for tension-compression under energy parameter control

No.	W_a, MJ/m^3	N_{exp}, cycles
1	0.30	173650
2	0.30	242850
3	0.40	64120
4	0.40	78440
5	0.55	19450
6	0.55	26530
7	0.70	13050
8	0.70	8120
9	0.85	4580
10	0.85	2900
11	1.00	1490
12	1.00	790
13	1.00	2700
14	1.15	820
15	1.15	830
16	1.30	585
17	1.30	485
18	1.45	380
19	1.45	420

The value of the constants found and the correlation coefficients are listed for models by Kandil's (see Eq. (4)), by Langer's (see Eq. (5)), and by the authors (see Eq.(6)) are listed in Tables 7, 8 and 9, respectively, while the corresponding fatigue life curves are shown in Figs. 6, 7, and 8, respectively.

As evident from the calculation analysis, the lowest scatter of experimental data was obtained for tension-compression with energy parameter control, and the largest one was for bending at controlled bending moment. By analysing the results of specific tests, it becomes clear that fatigue life is nearly identical across all tests; therefore, a combined fatigue life can be determined for each of the analysed models. The worst outcomes were obtained applying Langer's model. For that case, the combined fatigue strain-life curve cannot be applied. In the cases of Kandil's model and the authors' model, the scatter is very similar and those fatigue curves can be used in practice.

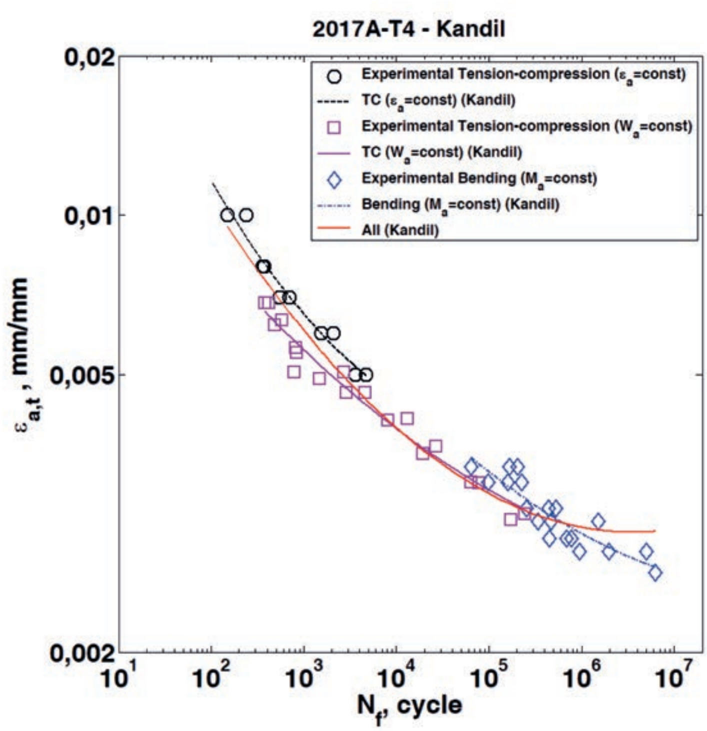

Fig. 6. Comparison of strain fatigue life according to Kandil's model – see Eq. (4)

Table 7. Summary of the parameters of analysed fatigue life curves according to Kandil's model – see Eq. (4)

Kandil				
	A	B	C	R^2
Tension-compression (ε_a=const)	-1.139	0.4945	0.04851	0.9554
Tension-compression (W_a=const)	-1.1611	0.2636	0.01642	0.9588
Bending (M_{ga}=const)	-1.283	0.3432	0.02059	0.7937
All (combined)	-1.305	0.3944	0.03007	0.9435

Table 8. Summary of the parameters of analysed fatigue life values according to Langer's model – see Eq. (5)

Langer				
	A	B	C	R^2
Tension-compression (ε_a=const)	-1.523	0.218	1.247	0.947
Tension-compression (W_a=const	-1.829	0.1407	0	0.9531
Bending (M_{ga}=const)	-1.949	0.1079	0	0.7823
All (combined)	-1.746	0.1516	0.001643	0.9082

Table 9. Summary of the parameters of analysed fatigue life values according to the authors' own model – see Eq. (6)

Authors					
	A	B	C	D	R^2
Tension-compression (ε_a=const)	-1.148	0.4847	0.04778	-0.00022	0.9554
Tension-compression (W_a=const)	-1.619	0.2675	0.01553	0.0003642	0.9585
Bending (M_{ga}=const)	-1.282	0.3432	0.02059	-0.0001049	0.7937
All (combined)	-1.29	0.4252	0.03083	0.0008263	0.9434

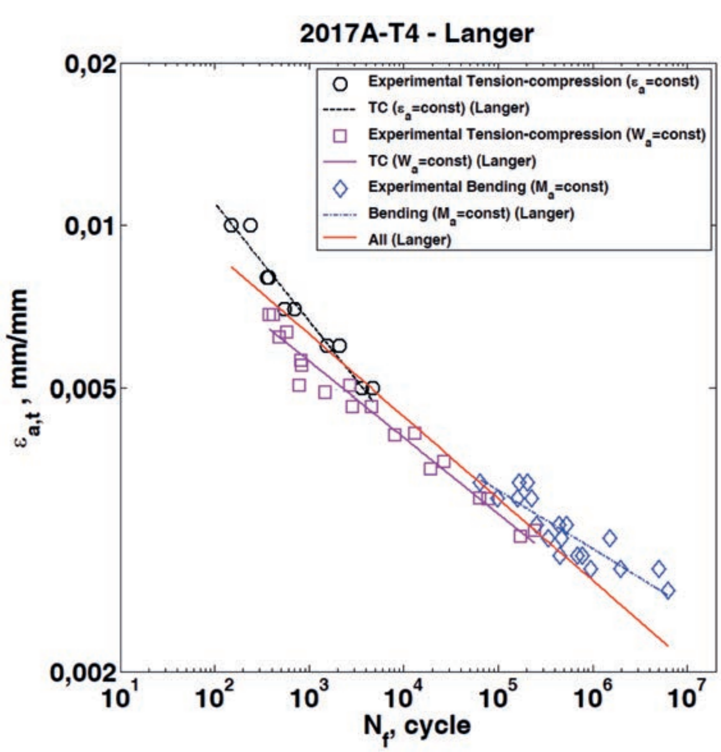

Fig. 7. Comparison of strain fatigue life according to Langer's model – see Eq. (5)

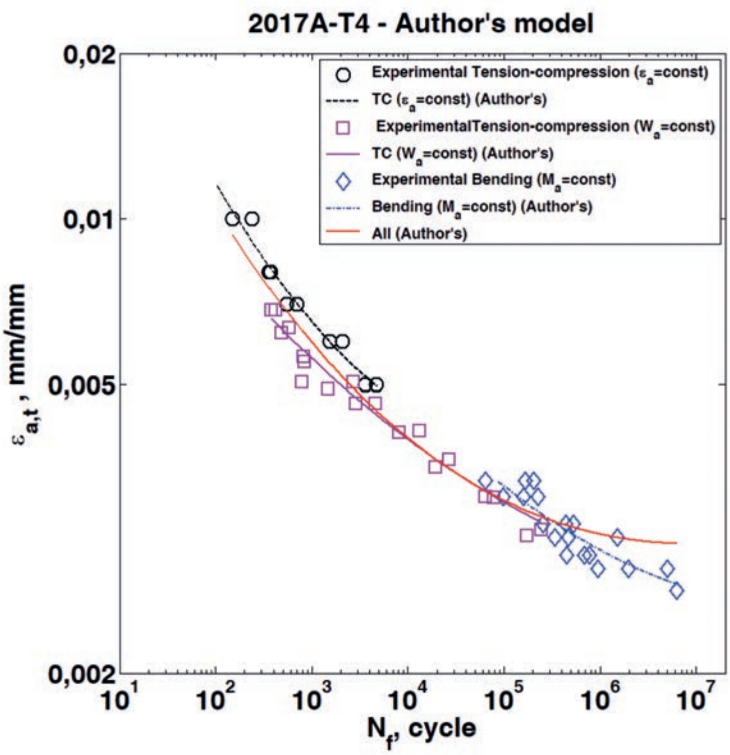

Fig. 8. Comparison of strain fatigue life according to the authors' own model – see Eq. (6)

Conclusions

As evident from the calculation analysis, the lowest scatter of experimental data was obtained for tension-compression with energy parameter control, and the largest scatter was for bending at controlled bending moment.

Analysing the results of specific tests, it becomes clear that fatigue life is almost identical across all tests; therefore, a common fatigue life can be determined for each of the analysed models.

The most unfavourable results were obtained applying Langer's model, while for Kandil's model and the authors' model, the scatter scale is similar.

Acknowledgements

This work has been carried out under the grant of National Science Centre (Poland) no. 2015/19/B/ST8/01115.

References

1. Achtelik H., Lachowicz C., Łagoda T., Macha E., 1997 Life time of the notched specimens of 10HNAP steel under proportional bending with torsion, in Proceedings and presented in 1st annual fatigue group meeting of Copernicus Contract CIPA CT940194, Smolenice – Słowacja, 17–18.11.1996, Editor M.Bily, Slovak Academy of Science, pp. 60–69
2. Manson S.S., Muralidharan U., 1987, Fatigue life prediction in bending from axial fatigue information, Fatigue Fract. Engng. Mater. Struct, Vol. 9, No 5, pp. 357–372.
3. Troschenko V., 1996, High-cycle fatigue and Inelasticity of Metals, Multiaxial and Fatigue Design, ESIS 21, (Edited by A.Pinueau, G.Cailletaud and T.C.Lindley), Mechanical Engineering Publications, London, pp. 335–348.
4. Megahed M.M., 1990, Prediction of bending fatigue behaviour by the reference stress approach, Fatigue Fract. Engng. Mater. Struct., Vol. 13, No 4, pp. 361–374.
5. Krzyżak D., Kurek M., Łagoda T. Sówka D., 2014, Influence of changes of the bending plane position on the fatigue life, Mat. – wiss. U. Werkstofftech., Vol. 45, No. 11 pp. 1018–1029.
6. Basquin O.H., (1910), The exponential law of endurance tests, Am. Soc. Test. Mater. Proc., Vol. 10, pp. 625–630.
7. Coffin L. F., (1954), A study of the effect of cyclic thermal stresses on a ductile metal, Trans ASME, Vol. 76, pp. 931–950.

8. Radhakrishnan V.M., 1992, On bilinearity of Manson-Coffin low-cycle-fatigue relationship, NASA Technical Memorandum 105840, p. 11.
9. Langer B.F., 1962, Design of Pressure Vessels for Low-Cycle Fatigue, ASME J. Basic Eng, Vol. 84, pp. 389–402.
10. Manson S.S, 1979, Inversion of the strain-life and strain-stress relationships for use in metal fatigue analysis, Fatigue of Engineering Materials and Structures, Vol. 1, pp. 37–57.
11. Manson S.S., 1965, Fatigue: A complex subject-some simple approximations, Experimental Mechanics, pp. 193–226.
12. Chopra O.K., 1999, Effects of LWR coolant environments of fatigue design curves of austenitic stainless steels, U.S. Nuclear Regulatory Commission.
13. Kandil F. A., 2000, The Determination of Uncertainties in Low Cycle Fatigue Testing, Standards Measurement & Testing Project No. SMT4-CT97-2165, Issue 1, pp. 1–26.
14. Gorash Y., Chen H., 2013, On creep-fatigue endurance of TIG-dressed weldments using the linear matching method, Engineering Failure Analysis, vol. 34, pp. 308–323.
15. Ramberg W., Osgood W. R., (1943), Description of stress-strain curves by three parameters, Technical Note No. 902, National Advisory Committee for Aeronautics, Washington DC.
16. Będkowski W., Łagoda T., Słowik J.: Strain controlled tests for determining the change of the material fatigue parameters, Materials Science, Vol.43, No. 4, 2007, pp. 492–498.
17. Kardas D., Kluger K., Łagoda T., Ogonowski P.: Fatigue life under proportional constant amplitude bending with torsion in energy approach basic on aluminium alloy 2017(a), Materials Science, Vol. 44, No. 4, 2008, pp. 541–549.
18. Walat K., Łagoda T., Lifetime of semi-ductile materials through the critical plane approach, Int. J. Fatigue, Vol. 67, 2014, pp.73–77.
19. Niesłony A., Łagoda T., Walat K., Kurek M., Multiaxial fatigue behaviour of AA6068 and AA2017A aluminium alloys under in-phase bending with torsion loading condition, Mat.-wiss. U. Werkstofftech, 45, vol. 45, No 10, pp. 947–952
20. Walat K., Łagoda T., Kurek M., Life time assessment of an aluminium alloy under complex low cycle fatigue loading, Materials Testing, vol. 57, 2015, pp.160–164.
21. Będkowski W., Słowik J., Badania zmęczeniowe stopu aluminium PA6 przy kontrolowanym parametrze gęstości energii odkształcenia, Raport Nr 1/WM/2004, Wydział Mechaniczny, Politechnika Opolska.
22. Łagoda T.: Energy models for fatigue life estimation under random loading – Part II – Verification of the model, Int. J. Fatigue, Vol. 23, 2001, No 6, pp. 481–489.